J. Cell. Mol. Med. Vol 13, No 5, 2009 pp. 948-958

Measuring and monitoring apoptosis and drug toxicity in HIV patients by ligation-mediated polymerase chain reaction

David J. Hooker [a, *], Paul R. Gorry [a, b, c], Anne M. Ellett [a], Steven L. Wesselingh [a, c, d], Catherine L. Cherry [a, c, d]

[a] Centre for Virology, Macfarlane Burnet Institute for Medical Research and Public Health, Melbourne, Victoria, Australia
[b] Department of Microbiology and Immunology, The University of Melbourne, Melbourne, Victoria, Australia
[c] Faculty of Medicine, Nursing and Health Sciences, Monash University, Melbourne, Victoria, Australia
[d] Infectious Diseases Unit, The Alfred Hospital, Melbourne, Victoria, Australia

Received: July 9, 2008; Accepted: October 30, 2008

Abstract

Apoptosis has a critical role in normal physiology while its dysregulation has causal links with certain pathologies. A biochemical hallmark of apoptosis, internucleosomal genomic DNA fragmentation, is detectable by ligation-mediated polymerase chain reaction (LM-PCR). Here we converted LM-PCR into a new apoptosis quantifier by dividing trace quantities of 600 bp apoptotic amplicons into those of a single copy house-keeping gene, generating the LM-PCR 'value'. Dynamic range was ~17-fold correlating with a ~200-fold difference in degree of apoptotic fragmentation. Inter- and intra-gel reliability were both excellent, supporting LM-PCR's utility with large sample sets. Validation experiments comprising cell exposure to staurosporine over time revealed LM-PCR is as sensitive as caspase-3/ELISA and more sensitive than terminal deoxynucleotidyl transferase-mediated dUTP nick end labelling/flourescence-activated cell sorting (TUNEL/FACS) for distinguishing low degrees of apoptosis (the spectrum most relevant *in vivo*). The LM-PCR profile mirrored that of caspase-3/ELISA but not TUNEL/FACS. We then applied this molecular tool to clinical investigation. Increased apoptosis is implicated in lipoatrophy (subcutaneous fat wasting), a serious, persistent toxicity of some nucleoside analogue reverse transcriptase inhibitors (NRTIs) used in anti-HIV highly active antiretroviral therapy (HAART). We demonstrated in 105 peripheral blood mononuclear cell samples that elevated LM-PCR values are seen during therapy with stavudine (d4T), a particularly toxic NRTI ($P < 0.0001$ *versus* no HAART, unpaired t-test). Elevated values were also independently associated with clinical evidence of lipoatrophy ($P = 0.007$, multiple logistic regression modelling) but not with patient age, CD4 T-cell count nor HIV viral load ($P > 0.8$ for each). Together these data demonstrate that LM-PCR is a robust and reliable quantifier of apoptosis with potential for basic science and clinical investigation.

Keywords: antiretroviral drugs • apoptosis • HAART • HIV-1 • ligation-mediated polymerase chain reaction • lipoatrophy • LM-PCR • NRTI • quantitation

Introduction

Apoptosis as a form of programmed cell death is a critical component of normal physiological processes such as immunity, embryogenesis and post-natal tissue development [1]. Regulation of apoptosis is essential for an organism's tissue homeostasis, while in human beings its dysregulation often correlates with pathological conditions such as carcinogenesis, myocardial ischemia, stroke, neurodegenerative diseases and acquired immune deficiency syndrome [2–8].

The cellular features of apoptosis are now well characterized and include loss of membrane attachment and symmetry, membrane blebbing and cytoplasmic and nuclear condensation. Intercommunicating molecular pathways [9] in human cells culminate in the activation of DNA fragmentation factor DFF-40/45 [10] and resultant internucleosomal cleavage of genomic DNA, visualized as a DNA 'ladder' by gel electrophoresis. The fact that DNA fragmentation is a terminal stage in the apoptotic process stamps it as a reliable indicator and an accepted hallmark of apoptosis [11–17].

Though apoptosis occurs *in vivo* and can be elevated in certain pathologies, the proportion of the genome that becomes

*Correspondence to: David J. HOOKER,
Macfarlane Burnet Institute for Medical Research and Public Health,
85 Commercial Road, Melbourne 3004, Australia.
Tel.: +61 3 85062345
Fax: +61 3 92822100
E-mail: dahoo@burnet.edu.au

doi:10.1111/j.1582-4934.2008.00612.x

fragmented over a given time is typically undetectable by electrophoresis. Using one form of ligation-mediated polymerase chain reaction (LM-PCR [18]), Staley *et al.* [15] detected apoptotic fragmentation in a wide range of invertebrate and vertebrate tissues. A sensitive assay not only detecting but quantifying this phenomenon would have value both in monitoring and understanding further the contribution of apoptotic dysregulation to disease processes. One aim here is to convert and validate LM-PCR for apoptosis quantification.

In HIV patients, highly active antiretroviral therapy (HAART) with nucleoside reverse transcriptase inhibitors (NRTIs) leads to serious and persistent toxicities including subcutaneous fat wasting (lipoatrophy) [19, 20] and peripheral neuropathy [21]. Lipoatrophy is particularly associated with exposure to stavudine [19], a drug that is pro-apoptotic *in vitro* and *in vivo* [22, 23]. The pathology of lipoatrophy in HIV patients includes increased adipocyte apoptosis [23]. One mechanism proposed for the elevated apoptosis seen in adipocytes is the interference of the mitochondria's role in apoptosis regulation by nucleoside analogue drugs inhibiting mitochondrial polymerase γ, an effect shown *in vitro* [24]. However, any link between NRTI toxicities in HIV patients and apoptosis in other tissues has not been well studied, and may be complicated by the pro-apoptotic effects of HIV itself [25–27]. Our aim here then is to investigate further the drug toxicities in HIV patients on HAART by applying LM-PCR to peripheral blood mononuclear cell (PBMC) genomic DNA from HAART-exposed and HAART-naïve patients from whom comprehensive clinical data are available. The development of LM-PCR as an apoptosis quantifier and its application here demonstrates its investigational potential for basic and clinical science.

Materials and methods

Cells and genomic DNA

PBMCs were collected at 6-month intervals from patients involved in a 2-year cohort study investigating the toxicity of antiretroviral therapies. This study was approved by the local Human Research and Ethics Committee and all subjects gave written, informed consent to participate. PBMCs from clinical samples were purified by Ficoll density gradient centrifugation (Invitrogen, Melbourne Australia; Amersham Biosciences, Uppsala, Sweden), solubilized in phosphate-buffered saline (PBS) with 0.4% sodium dodecyl sulphate (Amresco, OH, USA) and stored at –80°C. PBMCs used in validation experiments were purified from HIV-seronegative buffy coats packs by Ficoll density gradient centrifugation, cultured at 2×10^6 cells/ml and phytohaemagglutintin (Sigma-Aldrich, Castle Hill, Australia)-stimulated for 48 hrs in RPMI 1640 (Invitrogen), supplemented with 10% foetal bovine serum (batch tested for PBMC growth; Invitrogen), 1 U/ml penicillin and streptomycin (Invitrogen), 2 mM L-glutamine (Invitrogen) and 20 U/ml interleukin-2 (Roche, Sydney, Australia). Cultured Jurkat cells for validation experiments were grown at 1×10^6 cells/ml in RPMI 1640 supplemented with 10% foetal bovine serum, 1 U/ml penicillin and streptomycin and 2 mM L-glutamine. Genomic DNA was prepared from the above cell sources with Qiagen QIAamp DNA mini kits (Qiagen, Melbourne, Australia) and quantified spectrophotometrically in a Biophotometer (Eppendorf, Hamburg, Germany).

LM-PCR

LM-PCR [18] followed the procedure of Staley *et al.* [15] with modifications, and targeted the blunt-ended oligonucleosomal fragments of genomic DNA generated during apoptosis [11] – see Fig. 1. Genomic DNA was precipitated with 3 M sodium acetate pH 5.3 (Merck, Kilsyth, Victoria, Australia) and 100% ethanol (Merck), pelleted, washed and dried following established protocols [28] and redissolved in 10 mM Tris-HCl pH 8.0 (Reagent Organics, OH, USA) 0.5 mM ethylene diamine tetra-acetic acid (Pierce, IL, USA) ('T[E/2]') to 23.2 ng/μl.

A 12-μl annealing/ligation mixture was prepared containing genomic DNA at 16.7 ng/μl, 24mer and 12mer unphosphorylated oligonucleotide linkers ([15]; synthesized by Operon Biotechnologies, Cologne, Germany; Table 1) both at 20 pmol/μl, 50 mM Tris-HCl pH 7.6, 10 mM $MgCl_2$, 1 mM adenosine triphosphate (ATP), 1 mM dithiothreitol (DTT) and 5% polyethylene glycol (Invitrogen).

In this cocktail, the 24mer and 12mer were annealed to form blunt-ended partially double-stranded linkers by stepwise cooling from 55°C to 15°C in 5°C/8 min. increments then 10°C/20 min., employing a model PTC 200 DNA Engine (MJ Research, MA, USA). At the 10-min. point of 10°C the program was paused and 1.2 U T4 DNA ligase (Invitrogen, diluted to 1 U/μl in 200 mM Tris-HCl pH 7.6, 40 mM $MgCl_2$, 2 mM ATP and 4 mM DTT) was added, mixed and the temperature continued for 10°C/10 min. then ramped to 16°C/16 hrs for ligation to proceed.

After diluting the annealing/ligation reactions to 5 ng/μl DNA with T[E/2], 25 μl LM-PCR reactions were prepared containing 1.5 ng/μl DNA from the diluted annealing/ligation reaction, additional 24mer at 1.25 pmol/μl, 1× Taq DNA polymerase buffer (67 mM Tris-HCl pH 8.8, 16.6 mM $[NH_4]_2SO_4$, 0.45% Triton X-100, 200μg/ml gelatin; Fisher Biotech, Thebarton, Australia), 320 μM (each) dATP, dTTP, dGTP, dCTP, 2 mM $MgCl_2$ and 0.1 U/μl Taq polymerase (Fisher Biotech) as a Taq-antibody complex allowing a PCR hot-start. The Taq-antibody complex was prepared with 'Jumpstart' Taq antibody (Sigma-Aldrich, MO, USA) according to instructions, generating a complex at 0.83 (Taq)U/μl. LM-PCR reactions were heated in a DNA Engine to 94°C for 1 min. to activate Taq polymerase and remove 12mers, then ramped to 72°C for 4 min. to re-anneal the target DNA and generate complimentary sequence to the ligated 24mers. PCR then proceeded over 24 cycles (cultured cells) or 30 cycles (clinical sample PBMCs) of 94°C for 1 min. followed by annealing/extension at 72°C for 3 min., then completed with a single 72°C for 15 min. extension.

Though each LM-PCR reaction used comparable nanogram amounts of genomic DNA as starting material, more accurate sample-to-sample comparisons were generated by separate PCR reactions producing 239 bp amplicons specific to the single copy gene CCR5 [29]. Twenty-five microlitres 'CCR5' reactions comprised 1.5 ng/μl genomic DNA, 3 ng/μl each of primers LK46 and LK47 (Table 1), 1× Taq polymerase buffer (as for LM-PCR), 320 μM (each) dATP, dTTP, dGTP, dCTP and 3.5 mM $MgCl_2$. Reactions proceeded in a DNA Engine by initially heating to 94°C for 2 min., then 24 cycles (cultured cells) or 30 cycles (clinical sample PBMCs) of denaturation at 94°C for 30 sec., annealing at 60°C for 1 min., and extension at 72°C for 30 sec., and completed with a final extension at 72°C for 10 min.

After analytical 1.3% agarose gel electrophoresis of LM-PCR reactions and corresponding CCR5 reactions, inter-sample comparative quantitation was achieved by measuring trace quantity ethidium bromide fluorescence signals of 600 bp apoptotic bands relative to trace quantities of their

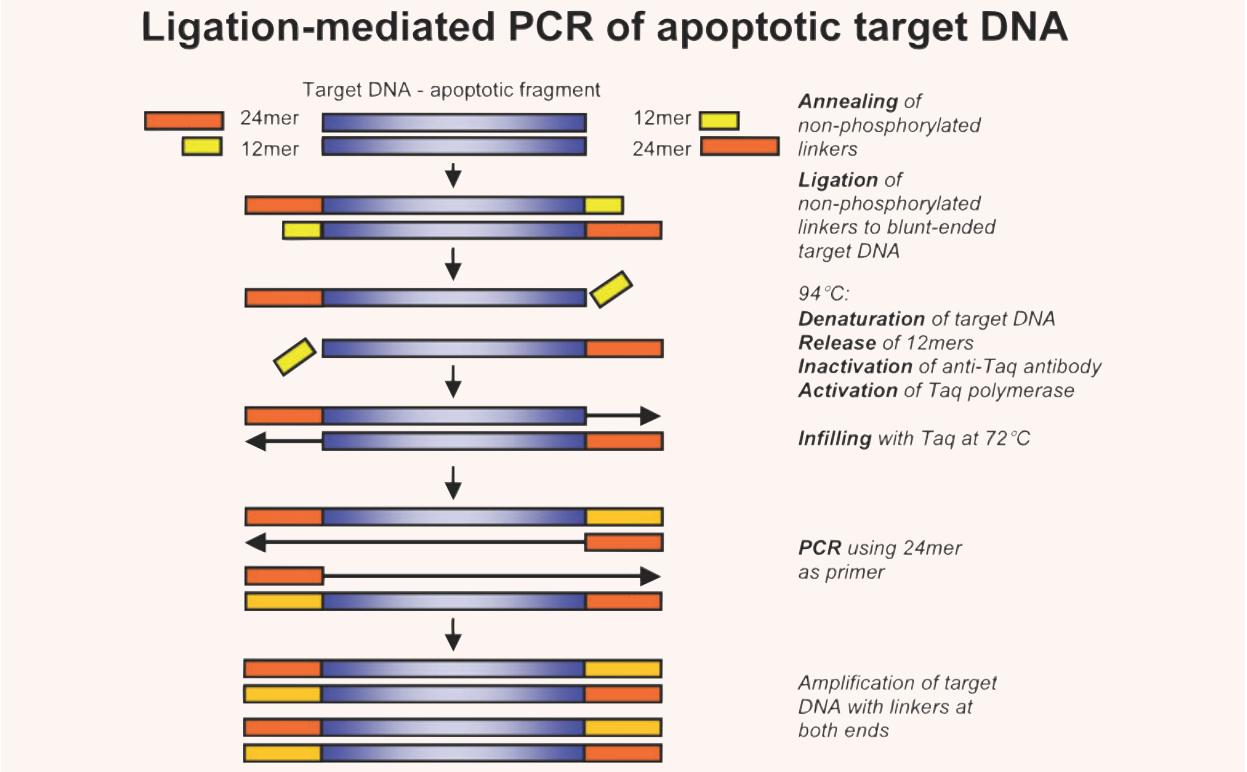

Fig. 1 LM-PCR steps for the amplification of blunt-ended target DNA. Modified from Staley *et al.* [15]. Blue boxes: single strands of target DNA; yellow boxes: 12mers; red and orange boxes: 24mers and their synthesized complement respectively. Modification involves an additional 94°C commencement step causing dissociation of Taq polymerase / Taq antibody complex and resultant activation of Taq polymerase and removal of 12mers, such that upon subsequent cooling to 72°C target DNA renatures without re-annealing of 12mers. Amplification is also given an additional single step for 15 min. at 72°C at the end of cycling to improve the level of complete synthesis by Taq polymerase.

Table 1 Oligonucleotides for LM-PCR

Oligonucleotide	Length	Sequence 5′ to 3′
LMPCR1	24	AGCACTCTCGAGCCTCTCACCGCA
LMPCR2	12	TGCGGTGAGAGG
LK46	24	GCTGTGTTTGCGTCTCTCCCAGGA
LK47	24	CTCACAGCCCTGTGCCTCTTCTTC

respective CCR5 amplicons using a Gel-Doc imager and Quantity One software (Bio-Rad Laboratories, Gladesville, New South Wales, Australia). This ratio was designated the LM-PCR value.

Controls

The target DNA for a positive LM-PCR reaction control consisted of a 396 bp blunt ended Pvu II fragment isolated from pT7T319U (a derivative of pUC19, Pharmacia Biotech, Uppsala, Sweden; [30]). Negative LM-PCR and CCR5 PCR controls were PCR-grade H_2O. Comparative quantitation of LM-PCR values was controlled from gel to gel for variations in ethidium bromide gel staining, destaining and photographic exposure, by reference to the sum trace quantities of 1000 bp, 850 bp, 650 bp and 500 bp bands from the molecular weight markers '1 Kb Plus DNA Ladder' (Invitrogen, Victoria, Australia) loaded on all agarose gels in equal amounts. Digital exposures were below the level of pixel saturation. To control for possible variations in LM-PCR product yield due to different Taq polymerase and Taq antibody batches, test samples on each gel were co-electrophoresed with three standards yielding low, mid and higher LM-PCR values. The sum of these standards for each gel were referenced back to the LM-PCR values of the same standards run using initial batches, and test LM-PCR values adjusted accordingly.

Measurement of apoptosis in cells exposed to staurosporine

PHA-stimulated PBMCs grown to log phase in the presence of 20 U/ml interleukin-2, and log-phase Jurkat cells, formed cultures that were separately exposed to staurosporine over time. In parallel, cells at 10^6/ml were incubated with 0, 0.1 or 0.5 μM staurosporine (Sigma-Aldrich, Castle Hill, NSW, Australia) [31–33] with cells removed and processed at 0, 1, 2, 3, 4 and 5 hrs. Three experiments for apoptosis measurement were then performed on the one cell pool at each time-point.

Terminal deoxynucleotidyl transferase-mediated dUTP nick end labelling/flourescence-activated cell sorting (TUNEL/FACS)

At each time-point 6 ml cells were collected, washed twice with PBS and resuspended in 300 μl PBS + 1% foetal bovine serum (PBMCs) or PBS (Jurkat cells) to 2×10^7 cells/ml for triplicate 100 μl cells per microwell. TUNEL procedure for cell suspensions followed the *In Situ* Cell Death Detection Kit, Flourescein (Roche, Mannheim, Germany) with the following modifications: after pelleting cells in wells, supernatant was aspirated and cells gently resuspended in 100 μl / well of fixation/permeabilization solution (Cytofix/Cytoperm kit, BD Biosciences/Pharmingen, CA, USA). After incubation for 20 min. at 4°C, cells were washed at this and subsequent wash stages two times at room temperature with perm/wash buffer (Cytofix/Cytoperm kit). After final washes cells were resuspended in 250 μl/well 1% paraformaldehyde in PBS, stored 4°C in the dark for up to 12 hrs and analysed by FACS at excitation 488 nm, detection 530 nm using a BD FACScan (BD Biosciences). At each measurement at least 10,000 events (PBMCs) or 15,000 events (Jurkat cells) were sorted.

Active caspase-3/ELISA

For each time-point 6 ml cells were harvested, washed twice with PBS, resuspended and solubilized in 500 μl cell lysis buffer (BD Pharmingen) and stored at −80°C. Separate aliquots of lysate were also stored at −80°C prior to protein estimation (in duplicate) using the Bio-Rad DC protein assay (Bio-Rad Laboratories). The ELISA followed BD Pharmingen's procedure in the 'human active caspase-3 ELISA pair technical data sheet', incorporating the pre-optimized components of purified mouse anti-human caspase-3 monoclonal capture antibody, purified rabbit anti-active caspase-3 monoclonal detection antibody, goat anti-rabbit horse radish peroxidase polyclonal antibody and tetramethylbenzidine substrate solution. Optical density measurements were confirmed in the linear range by performing duplicate reactions of 3 dilutions of lysate for each time-point. Modifications included blocking with 300 μl assay diluent (BD Pharmingen) per well and using a working dilution of horse radish peroxidase antibody at 1 in 2500. Blank consisted of assay diluent alone. Final optical density figures were obtained by first correcting $OD_{450\ nm}$ by subtracting $OD_{570\ nm}$ for all wells including blank, then subtracting corrected blank from corrected test samples.

LM-PCR

A total of 1.5 ml of cells at each time-point was washed once with PBS, resuspended in 200 μl PBS and stored at –80°C. Genomic DNA was then purified and subjected to LM-PCR. Three independent sets of annealing/ligation reactions, 24-cycle LM-PCR reactions and 24-cycle CCR5 reactions were completed for all time-points.

In order to more accurately compare LM-PCR values in this time course to active caspase-3 levels by ELISA, we converted LM-PCR values to fold-difference apoptotic fragmentation by first constructing an LM-PCR reference curve (Fig. 4). To construct this curve we diluted genomic DNA from one high-level LM-PCR value PBMC sample (LM-PCR value ~10), generating known graded amounts of 800, 400, 200 (the standard input amount), 100, 80, 60, 40, 20, 10, 5 and 2 ng in 12-μl annealing/ligation reactions. This range represented a 400-fold difference in apoptotic fragmentation. Mean LM-PCR values were generated from quadruple reactions for each dilution.

Statistical analysis

All statistical analyses were undertaken using Stata 9.2 (StataCorp, College Station, TX, USA). The tests used for each data set are described with the results.

Results

LM-PCR 'value', optimization, reproducibility and dynamic range

Employing trace quantity measurement of electrophoresed bands, we converted LM-PCR into a tool for quantification by dividing the 600 bp amplicon (Fig. 2A) of apoptosis into an amplicon formed by PCR of a single-copy 'house-keeping' gene (in this case, the CCR5 gene). Designated the LM-PCR value, this ratio reflected the amount of apoptosis per unit of standardized input genomic DNA, allowing comparative quantification.

The linkers designed for LM-PCR can amplify any blunt ended and possibly non-apoptotic fragment, and the background signal after LM-PCR can reveal non-oligonucleosomal sized fragments of broad random length. In order to confine measurement to a defined product of apoptosis, the discrete oligonucleosomal-sized populations were made the target for measurement. Gaussian modelling was not possible due to the shape and close proximity of apoptotic bands. Trace quantification was however highly reproducible. In our hands LM-PCR routinely generated a ladder from 200 to 1400 bp, a realistic representation of non-amplified apoptotic laddering. However, 200 bp exhibited highly variable inter-sample yields while levels diminished from 1000 bp and higher. The most robust and reproducible yields were observed at 400, 600 and 800 bp. The 600 bp band was at or near the peak of intensity levels and unlike the 400 bp band its trace was not occasionally merged with non-specific PCR product migrating near that region of the gel; it was therefore chosen as the band of choice for trace quantity measurement. Trace quantities of 400, 600 and 800 bp bands were totalled for 137 different LM-PCR reactions and plotted against 600 bp trace quantities for the same reactions (Fig. 2B). $R^2 = 0.99$, indicating the 600 bp band is a precise indicator of the intensity of amplified apoptotic fragmentation.

An anti-Taq antibody allowed multiple concurrent hot-start samples with better reproducibility than manual tube-by-tube addition [15] of Taq polymerase, and adapted LM-PCR for clinical investigation where large samples numbers are often screened. Disadvantages included a slightly but consistently reduced yield and the limitation to Taq polymerase, the only enzyme neutralized by this monoclonal antibody – though other higher fidelity and higher processivity polymerases (KlenTaq, Sigma; KODHotstart, Novagen; Immolase, Bioline) failed to generate amplified ladders in this system (data not shown).

A critical parameter for LM-PCR in its present form is that the target DNA be at least predominantly blunt ended [15].

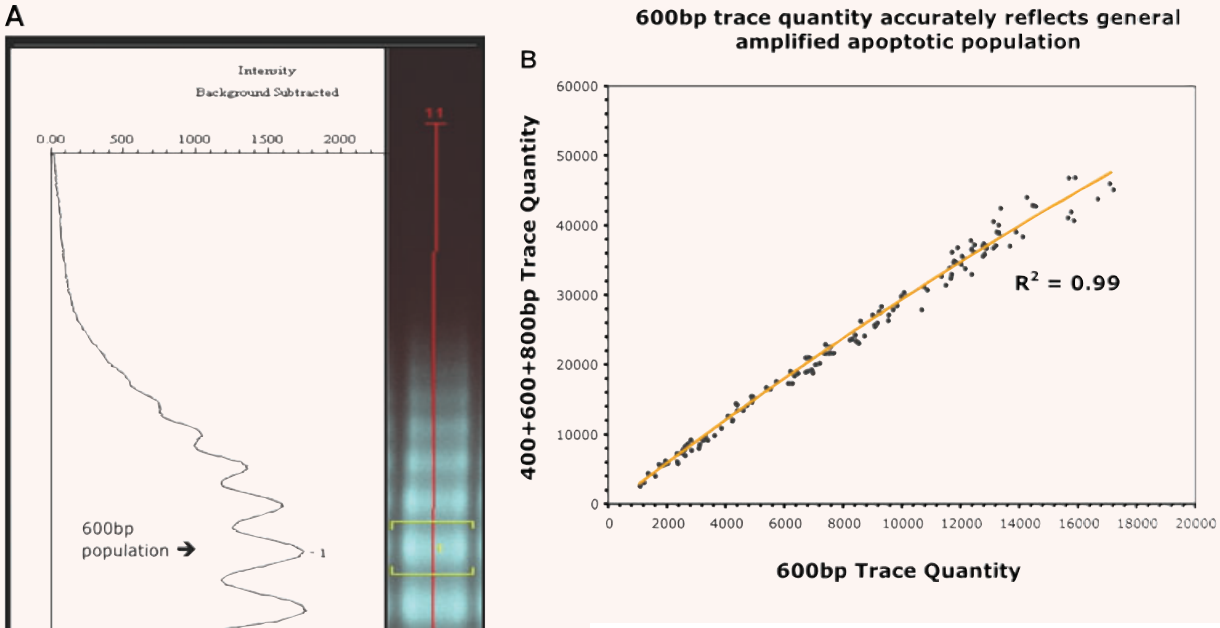

Fig. 2 (**A**) Example of apoptotic amplicons after LM-PCR, and resulting trace, with corresponding amplification of the 239 bp CCR5 amplicon. Trace quantity accounts for pixel number and intensity across the breadth and depth of amplicon populations. (**B**) Trace quantities of LM-PCR – amplified 600 bp apoptotic fragments plotted against the sum trace quantities of 400, 600 and 800 bp apoptotic fragments, using target DNA from 137 different PBMC genomic DNA preparations. $R^2 = 0.99$ indicating very strong correlation between 600 bp trace quantities and the sum quantities of 400, 600 and 800 bp.

Subsequent studies however have suggested that the active form of DFF-40, the endonuclease believed to be primarily responsible for internucleosomal cision, generates both 5′-phosphorylated blunt ends and ends with single 5′ overhangs with approximately equal frequency [34] (their Fig. 2). However, cleavage in this system derived not from the action of DFF-40 *in vivo* but from purified DFF-40 acting on plasmid restriction fragments *in vitro*. Considering nevertheless the possibility that the proportion of blunt and single base 5′-overhanging ends may vary in different systems, we designed new 13mers to replace the 12mers allowing single base cohesive end ligation to target DNA with 5′-overhangs, thus aiming to improve LM-PCR's ability to detect a greater proportion of apoptotic products. Adding the 13mers 50:50 with 12mers, we then proportioned them in LM-PCR reactions according to the relative frequency of purines and pyrimidines around the general site recognition sequence [34]. However, this failed to improve the yield of LM-PCR product, supporting Staley *et al.*'s observation.

To assess across a range of LM-PCR values the influence on reproducibility of the processes of scaled-down (12 μl) annealing/ligation reaction volumes, gel sample loading and trace quantity measurement of both LM-PCR and CCR5 reactions,

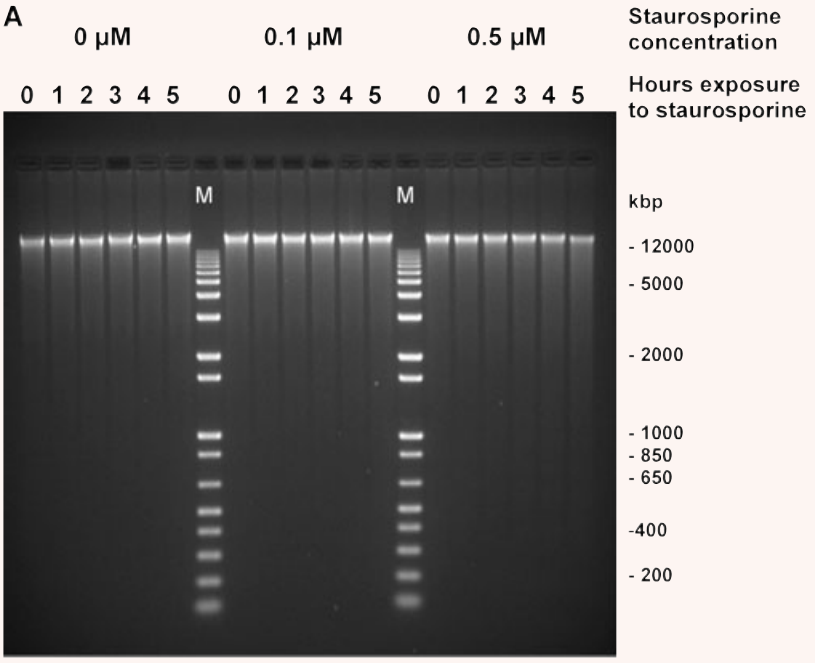

Fig. 3. (**A**) Non-LM-PCR'd genomic DNA from buffy coat PBMCs was prepared as described for each time-point and staurosporine concentration, 300 ng per track electrophoresed on 1.2% agarose gels then stained with ethidium bromide and destained. M: molecular weight markers. Under these conditions, apoptotic fragments were not visible by electrophoresis for all time-points and all staurosporine concentrations. (**B** to **G**) Three experiments in two cell types to validate LM-PCR by comparing the protocol with other systems of quantifying apoptosis. Diamonds, triangles and circles define shifts in values due to 0, 0.1 and 0.5 μM staurosporine, respectively. Error bars not visible fall within the dimensions of the graph symbols. (**B**) Changes in PBMC TUNEL-positivity with time as measured by FACS. Error bars are means +/−1 S.D., $n = 3$. (**C**) Changes in PBMC LM-PCR value with time. Error bars are means +/−1 S.D., $n = 3$. (**D**) Changes in Jurkat cell TUNEL-positivity with time. Error bars are means +/−1 S.D., $n = 3$. (**E**) Changes in Jurkat cell LM-PCR value with time. Error bars are means +/−1 S.D., $n = 3$. (**F**) Changes in Jurkat cell active caspase-3 levels with time as measured by horse radish peroxidase ELISA. An aberrant low reading at $t = 4$ hrs was due to loss of lysate only from those samples during ELISA. Error bars are means +/−1 S.D., $n = 2$. (**G**) Mean LM-PCR values from (**E**) converted to fold difference apoptotic fragmentation using the reference curve of Fig. 4.

LM-PCR reactions were generated from the PBMCs of two different blood samples, each reaction electrophoresed repeatedly on its own gel and trace quantities measured to generate multiple LM-PCR values. Sample 1: $n = 15$, mean = 1.33; sample 2: $n = 15$, mean = 2.40. The intra-class correlation coefficient (ICC, a measure of data consistency with a theoretical maximum value of 1) = 0.95 and the S.E.M. = 0.12, indicating excellent intra-assay reliability. To assess the influence on reproducibility of the processes of gel electrophoresis, band detection and digital image capture, three clinical genomic PBMC DNA samples that generate low, medium and higher level LM-PCR values were electrophoresed together on 12 separate gels on different days. LM-PCR values were also highly consistent between assays: ICC = 0.97 and S.E.M. = 0.17.

We have observed a 17-fold range (0.49 to 8.46) for LM-PCR values generated from clinical sample PBMCs and a similar range (0.36 to 8.20, 22-fold; Fig. 3E) in Jurkat cell culture exposed to 0.5 μM staurosporine. This latter range translates to a ~200-fold difference in apoptotic fragmentation as calculated from a reference curve (Fig. 4).

Validation of LM-PCR: In parallel with accepted procedures for measuring levels of apoptosis, LM-PCR measures increasing apoptosis with increasing exposure of cells to staurosporine

Utilising PBMCs and Jurkat cells we validated LM-PCR's ability to quantitatively compare apoptosis levels by comparing its measurement of apoptosis with apoptosis markers generated using two other accepted procedures, TUNEL [35] with measurement by FACS [36] and human active caspase-3 measurement by ELISA. TUNEL/FACS measures fluorescence of flourescein-dUTP incorporated at DNA strand breaks. The active form of caspase-3, now a widely accepted marker for apoptosis [37, 38], is quantified in cell lysates by horse radish peroxidase-mediated colorimetric change of the substrate tetramethylbenzidine. For each cell type, all apoptosis markers were measured from one cell pool at each time-point.

See Fig. 3A–G. Figure 3A reveals no visible fragmentation of non-LM-PCR'd PBMC genomic DNA at any time-point for all staurosporine concentrations, mimicking the typically low levels of

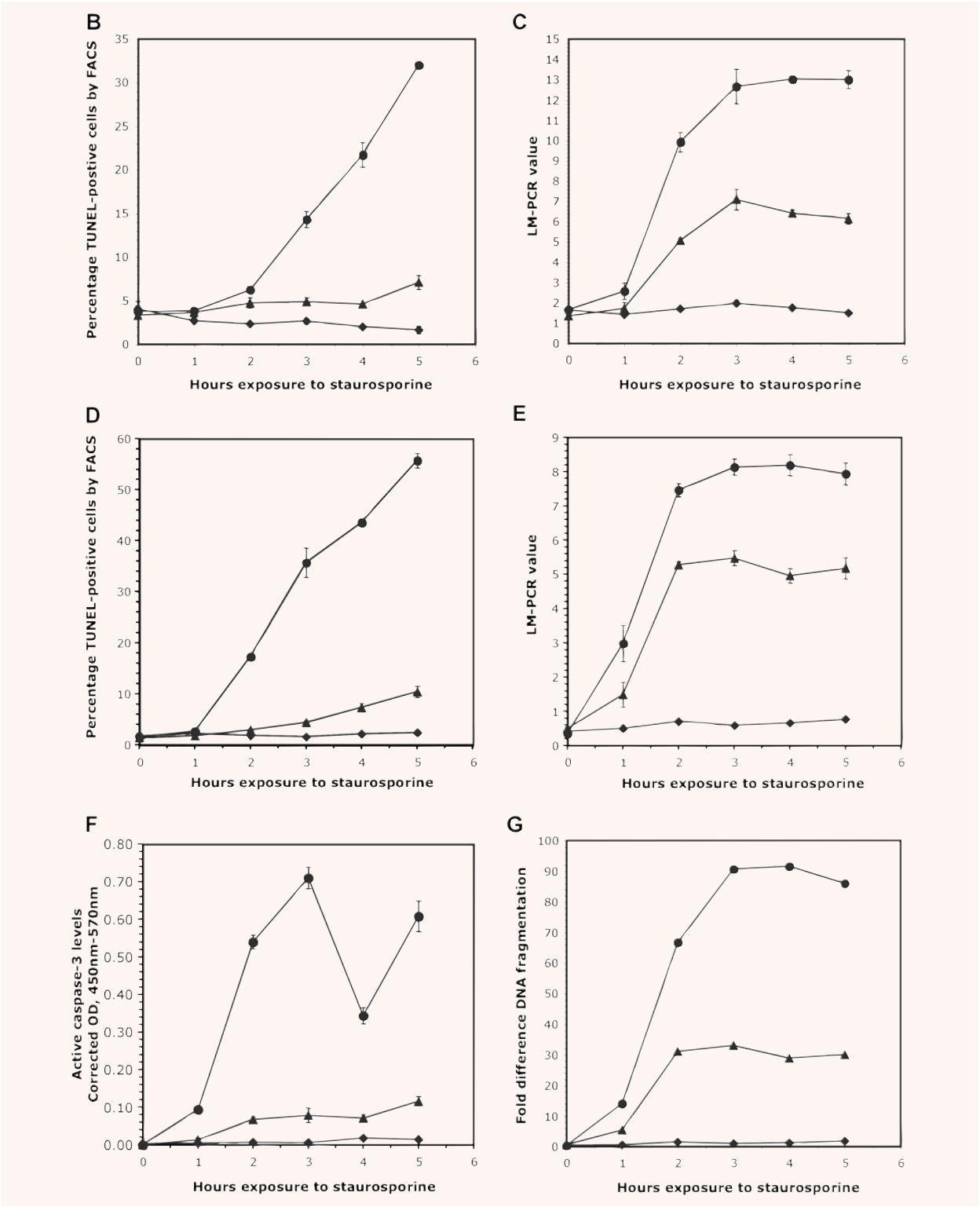

Fig. 3 Continued.

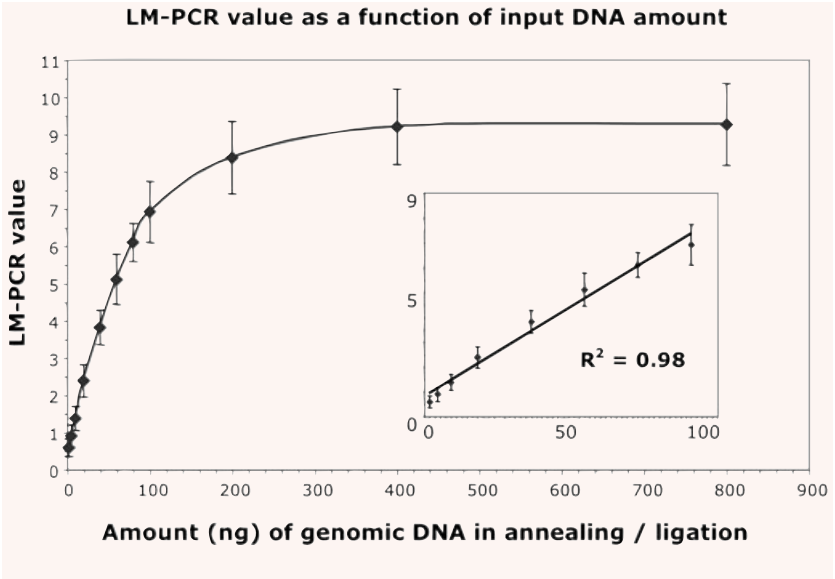

Fig. 4 To convert LM-PCR values to fold-difference fragmentation, a reference curve was constructed with LM-PCR values as a function of amount of genomic DNA in annealing/ligation reactions. The curve's value is based on the premise that because exactly the same sample has been used in all dilutions, the fold difference [amount genomic DNA] = fold difference [amount apoptotic DNA]. Genomic DNA from one high-level LM-PCR value PBMC sample (LM-PCR value ~10) was diluted to amounts of 800, 400, 200 (the standard input amount), 100, 80, 60, 40, 20, 10, 5 and 2 ng in 12-μl annealing/ligation reactions, and target DNA LM-PCR amplified over 24 cycles. Mean LM-PCR values were generated from quadruple reactions for each dilution. Error bars +/−1 S.D. Inset: same graph but with a restricted number of points showing near-linear correlation over a 50-fold range similar to the range seen with *in vivo* samples.

fragmentation seen in clinical sample genomic DNA. TUNEL/FACS and LM-PCR clearly distinguished between 0, 0.1 and 0.5 μM staurosporine time courses in both cell types. Active caspase-3/ELISA likewise distinguished these time courses in Jurkat cells, though was unable to quantify caspase levels in PBMCs due to high-level non-specific reactivity across multiple separately tested donors. The 0 μM staurosporine profiles confirmed that apoptotic elevation with 0.1 μM staurosporine is genuine and not attributable to a rise in basal apoptotic levels during cell culture incubation.

Though TUNEL/FACS documented a fairly linear elevation of strand breaks with time, it was less able than LM-PCR to distinguish between 0 and 0.1 μM effects: In PBMCs and Jurkat cells respectively the *fold-difference* TUNEL-positive cells by FACS between 0 and 0.1 μM values at 2 hrs was 2.0 and 1.6, rising to 4.4 and 4.4 by 5 hrs (Fig. 3B–E). Additionally, in both cell types, though the TUNEL/FACS 0.5 μM course showed clear elevation with time, it was less able than LM-PCR to distinguish between 0 and 0.5 μM apoptosis levels at $t = 1$ to 2 hrs (PBMCs) and $t = 1$ hr (Jurkat cells) (Fig. 3B–E). In Jurkat cells, both LM-PCR and caspase-3/ELISA were comparable in their ability to distinguish effects between 0 and 0.1 μM courses, both increasing their fold difference values from approximately 2.5 to 10 over 1 to 5 hrs (Fig. 3E, F).

In contrast to TUNEL, in Jurkat cells both LM-PCR and active caspase-3/ELISA measurements accelerated from between 1 and 2 hrs, reaching a plateau beyond the 3-hr mark (Fig. 3E, F). Both 0.1 and 0.5 μM curves exhibited this profile. Using a reference curve of LM-PCR value against fold-difference input DNA (Fig. 4), the mean LM-PCR values from this time course were converted to fold-difference fragmentation (Fig. 3G). The caspase and LM-PCR fold-difference profiles exhibited striking similarities; in particular there was an approximate 1:1 correlation between fold-differences fragmentation *versus* active caspase-3 levels, though LM-PCR may be more sensitive at detecting low apoptosis levels. The observation that both active caspase-3/ELISA and LM-PCR protocols produced this kind of response reflects the known correlation between activated caspase-3 levels and induction of DFF-40/45, the endonuclease responsible for internucleosomal cleavage of genomic DNA. This further validates the profile of LM-PCR as actually reflecting the progress of apoptosis in this time course, rather than an artefact of LM-PCR.

Application of LM-PCR: measuring and monitoring apoptosis and drug toxicity in HIV patients

We applied LM-PCR to 105 PBMC samples collected from 27 comprehensively characterized HIV-1^+ individuals (aged 33–68 yrs) involved in a cohort study. Up to five samples per patient were collected at 6-month intervals. Nine patients were not on antiretroviral therapy at study entry, of whom five commenced HAART during follow-up. Eighteen patients entered study on treatment with HAART that included at least one of stavudine or didanosine (dNRTIs, drugs associated with a high degree of mitochondrial toxicity). Ten patients switched therapy to a dNRTI-sparing regimen and 8 patients remained on stable therapy. We examined associations between LM-PCR values, current drug exposures, clinical evidence of lipoatrophy (present in 12 patients, including two cases of incident lipoatrophy on study), as well as $CD4^+$ T cell count, viral load and patient age. PBMC LM-PCR values ranged from 0.3 to 8.5 with a mean value of 2.2. Values were higher in samples collected during stavudine therapy (mean 3.0, $n = 39$) than at other times (mean 1.8, $n = 66$, $P = 0.0009$, linear regression clustered by patient). Samples collected from patients on HAART including dual dNRTI displayed the highest PBMC LM-PCR results (Fig. 5). PBMC LM-PCR values were lower following cessation of dNRTI in the 10 patients who switched off these drugs during study (median 1.5 *versus* 2.1, $P = 0.05$, Wilcoxon signed-rank test). We observed no associations between LM-PCR

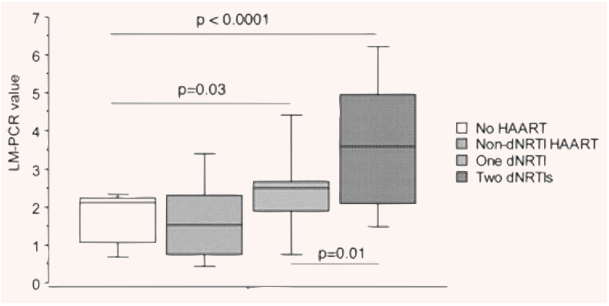

Fig. 5 LM-PCR values from 105 PBMC samples from 27 HIV-infected HAART+ and HAART- individuals. Samples collected at 6-month intervals with the following distribution: 30 samples collected while patients not on HAART, 27 collected during non-dNRTI HAART, 34 collected while on one dNRTI and 14 collected while on two dNRTI. Data here and in Figs 6 and 7 are represented as box-and-stem plots, in which boxes represent the median values and the second and third quartiles, and stems extend to the 10th and 90th percentiles. Outliers not shown but included in calculations. Patients on one dNRTI had higher PBMC LM-PCR values compared with those not on HAART ($P = 0.03$, anova). Patients using two dNRTIs had the highest LM-PCR values ($P < 0.0001$ *versus* no HAART, anova).

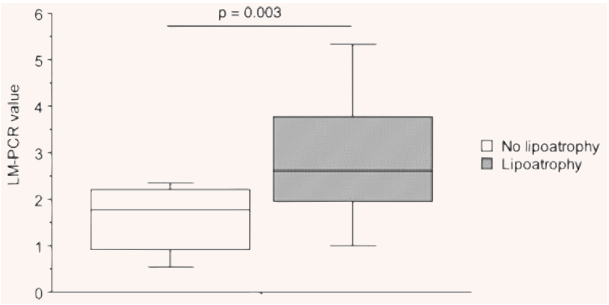

Fig. 6 LM-PCR values obtained from 105 PBMC samples from 27 HIV-infected individuals. Samples collected at 6-month intervals with the following distribution: 47 samples collected from patients having lipoatrophy (2 collected while patients not on HAART, 45 while on HAART), 58 samples from patients without lipoatrophy (27 not on HAART, 31 on HAART). Results were higher in samples collected from individuals with clinical evidence of lipoatrophy than those without (mean 3.0 *versus* 1.6, $P = 0.003$, linear regression clustered by patient).

values and $CD4^+$ T cell count, plasma HIV viral load or patient age ($P > 0.8$ for all).

Associations between PBMC LM-PCR values and clinical evidence of lipoatrophy were also examined. Elevated results were seen in samples from patients with lipoatrophy compared with those without (Fig. 6). Moreover, *within* the group of patients on stavudine at sample collection, LM-PCR values were significantly higher in samples from patients with lipoatrophy than those without (Fig. 7). Increasing patient age [39] and use of stavudine [19] are known risk factors for lipoatrophy. Logistic regression modelling confirmed that increasing PBMC LM-PCR value is associated with lipoatrophy independent of these factors (Table 2).

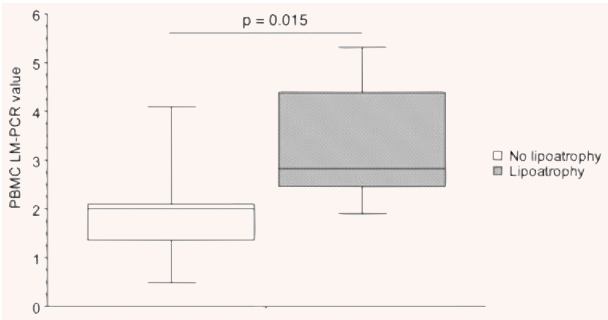

Fig. 7 LM-PCR values from 42 PBMC samples collected from 22 patients currently using stavudine. Samples collected at 6-month intervals with the following distribution: 12 samples from patients without lipoatrophy, 30 samples from patients having lipoatrophy. Patients on stavudine have higher PBMC LM-PCR results if they have lipoatrophy ($P = 0.015$, linear regression clustered by patient).

Table 2 Increasing PBMC LM-PCR value is associated with lipoatrophy independent of patient age and use of stavudine

Variable	Odds ratio	95% confidence interval	*P*-value
Current stavudine	5.5	1.7–17.8	0.004
LM-PCR value	2.2	1.2–3.9	0.007
Age (years)	1.1	1.0–1.2	0.09

Multiple logistic regression modelling confirms that increasing PBMC LM-PCR value is associated with lipoatrophy independent of patient age and use of stavudine. Overall model $P < 0.001$, $R^2 = 0.29$.

Discussion

Though LM-PCR exists in various guises [18, 40, 41], we have developed one form of LM-PCR into a new apoptosis quantifier, showing it to be reproducible and at least as sensitive as other accepted apoptosis quantifiers. This work is important because LM-PCR can assist in monitoring disease processes and in understanding the role of apoptosis in certain pathologies. Using this molecular tool, we have shown significant associations between PBMC LM-PCR values, exposure to NRTIs and clinical NRTI toxicity. We are currently evaluating associations with LM-PCR results in larger cohorts to extend these findings.

This assay has some advantages over other apoptosis quantifiers. It obviates the repeated need for viable cells and in contrast

works economically from a stable, consistent, easily stored, re-used and quantified form of one cell component – genomic DNA. It generates a value from a defined component of a hallmark of apoptosis, internucleosomal fragmentation, in contrast to histological and non-histological forms of TUNEL where apoptotic and non-apoptotic strand breaks may not be distinguished [42]. LM-PCR may also have an advantage over histological forms of TUNEL [35] when assaying for apoptosis in cells with unusually low nucleus:cell volume ratio; in the case of histological sections of adipocytes the few nuclei in view challenges quantitation [43]. LM-PCR can be applied to virtually any cell type from which sufficient (ng) quantities of genomic DNA can be isolated. It is appropriate when translating this tool to clinical investigation that LM-PCR measures apoptosis in cell *populations* because this is pertinent to the observation and implications of systemic effects. Additionally, as shown here LM-PCR appears to be more sensitive than TUNEL/FACS and as capable as caspase-3/ELISA at distinguishing different *low* levels of apoptosis, the kind of levels relevant to the clinical setting.

The sigmoid/plateau measurement profile observed here with both LM-PCR and active caspase-3 ELISA when measuring apoptosis in cell culture over time, has been observed by other investigators (BD Technical data sheet for human active caspase-3 ELISA pair, [35,31]) and may be typical of inducer-driven apoptosis under *in vitro* conditions. These observations further support the LM-PCR profile over the *in vitro* time course presented here as genuine rather than a limitation of LM-PCR itself.

Clinical sample genomic DNA rarely exhibits visible *non*-amplified fragmentation when electrophoresed. Therefore we were particularly interested to generate subtle shifts in apoptosis levels to the point where apoptosis was increasing yet non-amplified fragmentation was still not visible at the end of the time course, covering a typical *in vivo* range. To this end the 0- to 5-hr time courses with 0.1 and 0.5 μM staurosporine were successful. Over this clinically relevant range of levels LM-PCR was found to be particularly sensitive, supporting its use in the clinical setting. That apoptotic shifts at the low end of the spectrum is relevant to pathology is made clear when considering that for some tissues only 3% of total tissue mass need be apoptotic to generate tissue regression [44].

Elevated apoptosis in adipocytes has been associated previously with lipoatrophy and with dNRTI exposure, especially to didanosine and stavudine. Elevated myocyte apoptosis is also considered a possible mechanism in myopathy seen with exposure to another NRTI, zidovudine [45]. The molecular pathways underlying peripheral neuropathy are far less clear; theories explaining axonopathy involve both drug exposure and HIV infection [21, 46, 47]. To our knowledge our findings here form the first but preliminary report documenting significant elevation of apoptosis in PBMCs in association with dNRTIs and independent of plasma viral load, $CD4^+$ T cell count and patient age, further supporting dysregulation of apoptosis as a mechanism of NRTI toxicity. Significant association was also observed between elevated PBMC LM-PCR values and lipoatrophy: patients *on stavudine* have higher PBMC LM-PCR results *if* they have lipoatrophy. This supports the hypothesis that exposure to stavudine and didanosine are elevating apoptosis in a cell type other than adipocytes.

We have designed LM-PCR to quantify apoptosis on small quantities of genomic DNA, showing the assay to be robust, reliable and valid. Our work in the context of clinical and drug toxicity in HIV patients supports the potential utility of this assay for measuring and monitoring apoptosis in contexts other than HIV research in both basic science and clinical investigation.

Acknowledgements

This work was supported by a grant from The Australian Centre for HIV and Hepatitis Research (ACH2).

Disclosure/Duality of Interest

The authors declare that there is no duality of interest.

References

1. **Vaux DL, Korsemeyer SJ.** Cell death in development. *Cell.* 1999; 96: 245–54.
2. **Burns TF, El-Deiry W.** Cell death signalling in malignancy. *Cancer Treat Res.* 2003; 115: 319–43.
3. **Daniel PT, Weider T, Sturm I, Schulze-Osthoff K.** The kiss of death: promises and failures of death receptors and ligands in cancer therapy. *Leukemia.* 2001; 15: 1022–32.
4. **Ozoren N, El-Deiry W.** Cell surface death receptor signaling in normal and cancer cells. *Semin Cancer Biol.* 2003; 13: 135–47.
5. **Sheikh MS, Huang Y.** Death receptors as targets of cancer therapeutics. *Curr Drug Targets.* 2004; 4: 97–104.
6. **Thompson CB.** Apoptosis in the pathogenesis and treatment of disease. *Science.* 1995; 267: 1456–62.
7. **Zörnig M, Hueber A, Baum W, Evan G.** Apoptosis regulators and their role in tumorigenesis. *Biochim Biophys Acta.* 2001; 1551: F1–37.
8. **Green DR, Evan G.** A matter of life and death. *Cancer Cell.* 2002; 1: 19–30.
9. **Khosravi-Far R, Degli Esposti M.** Death receptor signals to mitochondria. *Cancer Biol Ther.* 2004; 3: 1051–7.
10. **Liu X, Li P, Widlak P, Zou H, Luo X, Garrard WT, Wang X.** The 40-kDa subunit of DNA fragmentation factor induces DNA fragmentation and chromatin condensation during apoptosis. *Proc Natl Acad Sci USA.* 1998; 95: 8461–6.
11. **Kerr JFR, Harmen BV.** Definition and incidence of apoptosis, an historical perspective. In: Tomei LD, Cope FO, editors. Apoptosis: the molecular basis of cell death. New York: Cold Spring Harbor Laboratory Press; 1991. pp. 5–29.
12. **Kerr JFR, Searle J, Harmen BV, Bishop CJ.** Apoptosis. In: Potten CS, editor. Perspectives on mammalian cell death. Oxford: Oxford University Press; 1987. pp. 93–128.
13. **Martz E, Howell DM.** CTL: virus controls cells first and cytolytic cells second? DNA

fragmentation, apoptosis and the prelytic halt hypothesis. *Immunol Today.* 1989; 10: 79–86.

14. **Shi Y, Szalay MG, Paskar L, Boyer M, Sigh B, Green DR.** Activation-induced cell death in T cell hybridomas is due to apoptosis. *J Immunol.* 1990; 144: 3326–33.
15. **Staley K, Blaschke AJ, Chun J.** Apoptotic DNA fragmentation is detected by a semiquantitative ligation-mediated PCR of blunt DNA ends. *Cell Death Differ.* 1997; 4: 66–75.
16. **Tian Q, Streuti M, Siato H, Schlossman SF, Anderson P.** A polyadenylate binding protein localized to the granules of cytolytic lymphocytes induces DNA fragmentation in target cells. *Cell.* 1991; 67: 629–39.
17. **Wyllie AH, Morris RG, Smith AL, Dunlop D.** Chromatin cleavage in apoptosis: association with condensed chromatin morphology and dependence on macromolecular synthesis. *J Pathol.* 1984; 142: 67–77.
18. **Mueller PR, Wold B.** In vivo footprinting of a muscle specific enhancer by ligation-mediated PCR. *Science.* 1989; 246: 780–6.
19. **Mallal S, John M, Moore C, James I, McKinnon E.** Contribution of nucleoside analogue reverse transcriptase inhibitors to subcutaneous fat wasting in patients with HIV infection. *AIDS.* 2000; 14: 1309–16.
20. **Bernasconi E, Boubaker K, Junghans C, Flepp M, Furrer HJ, Haensel A, Hirschel B, Boggian K, Chave JP, Opravil M, Weber R, Rickenbach M, Telenti A.** Abnormalities of body fat distribution in HIV-infected persons treated with antiretroviral drugs: The Swiss HIV Cohort Study. *J Acquir Immune Defic Syndr.* 2002; 31: 50–5.
21. **Cherry CL, McArthur JC, Hoy JF, Wesselingh SL.** Nucleoside analogues and neuropathy in the era of HAART. *J Clin Virol.* 26; 2003: 195–207.
22. **Caron M, Auclair M, Lagathu C, Lombes A, Walker UA, Kornprobst M, Capeau J.** The HIV-1 nucleoside reverse transcriptase inhibitors stavudine and zidovudine alter adipocyte functions *in vitro*. *AIDS.* 2004; 18: 2127–36.
23. **Cherry CL, Lal L, Thompson KA, McLean CA, Ross LL, Hernandez J, Wesselingh SL, McComsey G.** Increased adipocyte apoptosis in lipoatrophy improves within 48 weeks of switching therapy from stavudine to abacavir or zidovudine. *J Acquir Immune Defic Syndr.* 2005; 38: 263–7.
24. **Martin JL, Brown CE, Matthews-Davis N, Reardon JE.** Effects of antiviral nucleoside analogs on human DNA polymerases and mitochondrial DNA synthesis. *Antimicrob Agents Chemother.* 1994; 38: 2743–9.
25. **Groux H, Torpier G, Monte D, Mouton Y, Capron A, Ameisen C.** Activation-induced death by apoptosis in CD4+ T cells from human immunodeficiency virus-infected asymptomatic individuals. *J Exp Med.* 1992; 175: 331–40.
26. **Yue FY, Kovacs CM, Dimayuga RC, Gu XXJ, Parks P, Kaul R, Ostrowski MA.** Preferential apoptosis of HIV-1-specific CD4+ T cells. *J Immunol.* 2005; 174: 2196–204.
27. **Kaul M, Zheng J, Okamoto S, Gendelman HE, Lipton SA.** HIV-1 infection and AIDS: consequences for the central nervous system. *Cell Death Differ.* 2005; 12: 878–92.
28. **Sambrook J, Russell DW.** Molecular cloning, a laboratory manual. 3rd ed. Cold Spring Harbor, New York: Cold Spring Harbor Laboratory Press; 2001.
29. **Zhang L, Lewin SR, Markowitz M, Lin H-H, Skulsky E, Karanicolas R, He Y, Jin X, Tuttleton S, Vesanen M, Spiegel H, Kost R, Lunzen J, Stellbrink H-J, Wolinsky S, Borkowsky W, Palumbo P, Kostrikis LG, Ho DD.** Measuring recent thymic emigrants in blood of normal and HIV-1-infected individuals before and after effective therapy. *J Exp Med.* 1999; 190: 725–32.
30. **Olkkonen V, Gottleib M, Strassman PJ, Qiao X, Bamford DH, Mindich L.** In vitro assembly of infectious nucleocapsids of bacteriophage 6: formation of a recombinant double-stranded RNA virus. *Proc Natl Acad Sci USA.* 1990; 87: 9173–7.
31. **Stepczynska A, Lauber K, Engels IH, Janssen O, Kabelitz D, Wesselborg S Schulz-Osthoff K.** Staurosporine and conventional anticancer drugs induce overlapping, yet distinct pathways of apoptosis and caspase activation. *Oncogene.* 2001; 20: 1193–202.
32. **Jarvis WD, Turner AJ, Povirk LF, Traylor RS, Grant S.** Induction of apoptotic DNA fragmentation and cell death in HL-60 human promyelocytic leukemia cells by pharmacological inhibitors of protein kinase C. *Cancer Res.* 1994; 54: 1707–14.
33. **Nakadate T, Jeng AY, Blumberg PM.** Comparison of protein kinase C functional assays to clarify mechanisms of inhibitor action. *Biochem Pharmacol.* 1988; 37: 1541–2.
34. **Widlak P, Li P, Wang X, Garrard WT.** Cleavage preferences of the apoptotic endonuclease DFF40 (caspase activated DNase or nuclease) on naked DNA and chromatin substrates. *J Biol Chem.* 2000; 275: 8226–32.
35. **Gavrieli Y, Sherman Y, Ben-Sasson SA.** Identification of programmed cell death *in situ via* specific labeling of nuclear DNA fragmentation. *J Cell Biol.* 1992; 119: 493–501.
36. **Sgonc R, Boeck G, Dietrich H, Gruber J, Recheis H, Wick G.** Technical tips. *Trends genet.* 1994; 10: 41–2.
37. **Nicholson DW, Ali A, Thornberry NA, Vaillancourt JP, Ding CK, Gallant M, Gareau Y, Griffin PR, Labelle M, Lazebnik YA, Munday NA, Raju SM, Smulson ME, Yamin T-T, Yu VL, Miller DK.** Identification and inhibition of the ICE/CED-3 protease necessary for mammalian apoptosis. *Nature.* 1995; 376: 37–43.
38. **Patel T, Gores GJ, Kaufmann SH.** The role of proteases during apoptosis. *FASEB J.* 1996; 10: 587–97.
39. **McComsey G, Maa J-F.** Host factors may be more important than choice of antiretrovirals in the development of lipoatrophy. *AIDS Reader.* 2003; 13: 539–42.
40. **Masny A, Pluciennicz A.** Ligation-mediated PCR performed at low denaturation temperatures – PCR melting profiles. *Nuc Acids Res.* 2003; 31: e114.
41. **Guilfoyle RA, Leeck CL, Kroening D, Smith LM, Guo Z.** Ligation-mediated PCR amplification of specific fragments from a class-II restriction endonuclease total digest. *Nuc Acids Res.* 1997; 25: 1854–58.
42. **Yasuda M, Umemura S, Osamura RY, Kenjo T, Tsutsuni Y.** Apoptotic cells in the human endometrium and placental villi: pitfalls in applying the TUNEL method. *Arch Histol Cytol.* 1995; 58: 185–90.
43. **Domingo P, Matias-Guiu X, Pujol RM, Francia E, Lagarda E, Sambeat MA, Vazquez G.** Subcutaneous adipocyte apoptosis in HIV-1 protease inhibitor-associated lipodystrophy. *AIDS.* 1999; 13: 2261–7.
44. **Bursch W, Kleine L, Tenniswood M.** The biochemistry of cell death by apoptosis. *Biochem Cell Biol.* 1990; 68: 1071–4.
45. **Scruggs ER, Dirks Naylor AJ.** Mechanisms of zidovudine-induced mitochondrial toxicity and myopathy. *Pharmacology.* 2008; 82: 83–8.
46. **Robinson B, Li Z, Nath A.** Nucleoside reverse transcriptase inhibitors and human immunodeficiency virus proteins cause axonal injury in human dorsal root ganglion cultures. *J Neurovirol.* 2007; 13: 160–7.
47. **Cherry CL, Wesselingh SL.** Nucleoside analogues and HIV: the combined cost to mitochondria. *J Antimicrob Ther.* 2003; 51: 1091–3.